Phase transition, structural and thermodynamic properties of Mg_2Si polymorphs*

Yu Ben-Hai(余本海) and Chen Dong(陈 东)†

College of Physics and Electronic Engineering, Xinyang Normal University, Xinyang 464000, *China*

(Received 14 August 2010; revised manuscript received 16 September 2010)

The plane-wave pseudo-potential method within the framework of first principles is used to investigate the structural and elastic properties of Mg_2Si in its intermediate pressure ($Pnma$) and high pressure phases ($P6_3/mmc$). The lattice constants, the band structures. The bulk moduli of the Mg_2Si polymorphs are presented and discussed. The phase transition from anti-cotunnite to Ni_2In-type Mg_2Si is successfully reproduced using a vibrational Debye-like model. The phase boundary can be described as $P = 24.02994 + 3.93 \times 10^{-3}T - 4.66816 \times 10^{-5}T^2 - 2.2501 \times 10^{-9}T^3 + 2.33786 \times 10^{-11}T^4$. To complete the fundamental characteristics of these polymorphs we have analysed thermodynamic properties, such as thermal expansion and heat capacity, in a pressure range of 0–40 GPa and a temperature range of 0–1300 K. The obtained results tend to support the available experimental data and other theoretical results. Therefore, the present results indicate that the combination of first principles and a vibrational Debye-like model is an efficient scheme to simulate the high temperature behaviours of Mg_2Si.

Keywords: semiconductors, thermodynamic properties, phase transition, band structure
PACS: 05.70.Fh, 65.40.Ba, 71.15.Dx, 73.20.At **DOI:** 10.1088/1674-1056/20/3/030508

1. Introduction

Recently, semiconducting metal silicides have attracted much attention for their potential to create a new class of environmentally conscious electronics.[1] Due to its superior features such as low electrical resistivity, large Seebeck coefficient and low thermal conductivity, the Mg_2Si compound can be used as a thermoelectric power generator material with a maximum operating temperature of around 800 K, hence its important role in high temperature applications.[2−5] Numerous authoritative papers have been published regarding the fundamental electronic and optical properties of this compound.[6−9] Magnesium silicide is well known as a light material used in the automobile and aerospace industries due to its high specific strength and high specific elastic modulus.[10,11] As a stable compound,[12] Mg_2Si can also be used for optical fibres due to its good ohmic contact character with n-type Si.[13]

With the same structure, alkali-metal oxides and sulfides, Li_2O, Na_2S, K_2S, Li_2S and Rb_2S, have all been predicted or shown to adopt the same phase transition: anti-fluorite ($Fm\text{-}3m$)→ anti-cotunnite ($Pnma$) → Ni_2In-type ($P6_3/mmc$).[14−17] For Mg_2Si polymorphs, no further high-pressure experiment has been reported since Cannon and Conlin.[18] Recently, Hao *et al.*[19] experimentally determined the intermediate pressure phase and the high pressure phase of Mg_2Si, i.e., anti-cotunnite structure and Ni_2In-type structure.[20] In their work, the transition pressure was found to be 21.3 GPa. In Ref. [21], some thermodynamic properties of anti-fluorite Mg_2Si have been measured in a temperature range of 288 K–573 K. Tani and Kido[22] and Wang *et al.*[23] have investigated the ground state structural property and the elastic property of the same compound. Some thermal quantities such as entropy, heat capacity, thermal conductivity and Debye temperature were determined in a temperature range of 0–1300 K. However, in these papers no pressure effects were considered. The phase boundary from an anti-cotunnite structure to a Ni_2In-type structure is still unclear and some fundamental quantities, such as high-pressure elastic modulus, thermal expansion, heat capacity and bulk modulus for anti-cotunnite and Ni_2In-type Mg_2Si, are far from being complete. The phase transition of Mg_2Si has attracted significant attention from scientists due to its impor-

*Project supported by the National Natural Science Foundation of China (Grant Nos. 11005088 and 11047186), the Basic and Advanced Technology of Henan Province, China (Grant No. 102300410241), and the Science and Technology of Henan Province, China (Grant No. 082300410050).

†Corresponding author. E-mail: chchendong2010@163.com

© 2011 Chinese Physical Society and IOP Publishing Ltd

tance for understanding the dynamics of this compound. Therefore, an accurate investigation of the high-pressure structural parameter, the elastic modulus, the thermal property and the phase transition characteristics of Mg_2Si is highly required.

The aim of this paper is twofold: (1) to highlight the structural and elastic properties of anti-cotunnite and Ni_2In-type Mg_2Si; and (2) to provide the vibrational properties and phase boundary of Mg_2Si. In Section 2, the computational details are presented. Then, the computed results of structure, elastic modulus, thermal property and the phase boundary are discussed in Section 3. Finally, conclusions are drawn in Section 4.

2. Computational method

At intermediate pressure, Mg_2Si crystallizes in the anti-cotunnite structure (orthorhombic system, space group *Pnma*). There are eight Mg and four Si atoms in a unit cell. These atoms occupy the Mg1 (0.0306, 0.25, 0.1644), the Mg2 (0.1411, 0.25, 0.2608) and the Si (0.2527, 0.25, 0.8754) sites.[19] At high pressure, Mg_2Si has a Ni_2In-type structure (space group $P6_3/mmc$). Different atoms occupy the Mg1 (0.66666667, 0.33333333, 0.25), the Mg2 (0, 0, 0) and the Si (0.66666667, 0.33333333, 0.75) sites.[24] The crystal structures of anti-cotunnite and Ni_2In-type Mg_2Si are shown in Fig. 1. The crystal cell of anti-fluorite Mg_2Si is systemically discussed in our previous paper.[25]

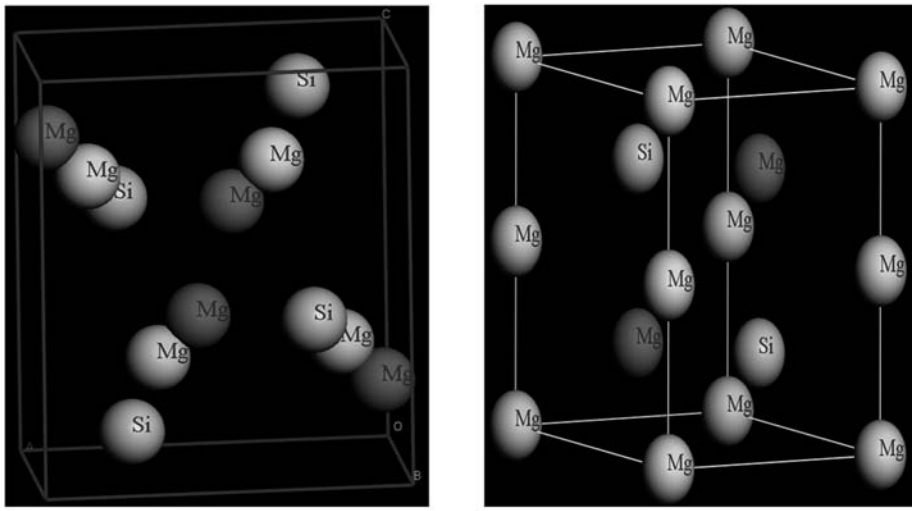


Fig. 1. Schematic unit cells used for anti-cotunnite Mg_2Si (a) and Ni_2In-type Mg_2Si (b).

The self-consistent total energy calculations are carried out using the plane-wave pseudopotential (PW-PP) method.[26] Here we employ the non-local ultrasoft pseudo-potentials introduced by Vanderbilt.[27] Exchange and correlation potentials are treated in the generalized gradient approximation (GGA) of Perdew–Burke–Ernzerhof (PBE) form.[28] Pseudo-atomic calculations are performed for Mg-$2p^6 3s^2$ and Si-$3s^2 3p^2$. The energy cutoffs are chosen to be 500 eV and 480 eV for Ni_2In-type and anti-cotunnite structures, respectively. The integration over the Brillouin zone is performed on a grid of special k points determined according to the Monkhorst–Pack scheme[29] ($15\times15\times10$ girds for Ni_2In-type Mg_2Si and $7\times9\times6$ girds for anti-cotunnite Mg_2Si). For the anti-cotunnite Mg_2Si crystal, the internal coordinates of all atoms are fully optimized. For both crystals, the self-consistent convergence of the total energy is 5×10^{-7} eV/cell. The lattice dynamics of the anti-fluorite Mg_2Si is studied by the linear response method.[30] This method allows us to avoid the need to construct a supercell, so calculations are done within a single unit cell. The q meshes for the Brillouin zone are sampled to $9\times9\times9$ for a cubic lattice.

Then, the recently developed vibrational Debye-like model[31] is used to calculate the equation of state (EOS) and the chemical potential that is constructed from the Helmholtz free energy. In this method, the phonon contributions and anharmonic effects are also considered. The isotropic approximation is used to

determine the Debye temperature, given as

$$\theta_{\rm D} = \frac{h}{2\pi}(6\pi^2 V^{1/2} n)^{1/3} f(\sigma)\sqrt{\frac{B_{\rm S}}{k_{\rm B}^2 M}}, \qquad (1)$$

where V, M, n, $B_{\rm S}$, $f(\sigma)$ and $k_{\rm B}$ are the primitive cell volume, molar mass, number of atoms per unit cell, adiabatic bulk modulus, the scaling function that depends on the Poisson ratio σ of the isotropic solid and the Boltzman constant, respectively. A simple way to use the Debye model is to consider that the adiabatic bulk modulus $B_{\rm S}$ is equal to the isothermal bulk modulus $B_{\rm T}$, leading to the following equation:

$$B_{\rm S} \approx B_{\rm T} = V\left(\frac{{\rm d}^2 E}{{\rm d}V^2}\right), \qquad (2)$$

where E is the total energy. Using the calculated energy–volume data points (E–V data), the vibrational Debye-like model allows one (a) to calculate the Debye temperature from Eqs. (1) and (2), and (b) to obtain the non-equilibrium Gibbs energy $G^*(V;p,T)$

$$G^*(V;p,T) = E(V) + pV + A_{\rm vib}(T,\theta_{\rm D}(V)), \qquad (3)$$

where $E(V)$ is the total energy per unit cell; the second term on the right-hand side, PV, corresponds to the constant hydrostatic pressure condition; the third term, $A_{\rm vib}$, is the vibrational Helmholtz free energy. Series standard thermodynamic relations are determined by fitting the calculated E–V data points to the second order Birch–Murnaghan EOS[32]

$$P = 3B_0 f_E(1+2f_E)^{5/2}\left[1+\frac{3}{2}(B'-4)f_E + \frac{3}{2}\left(B_0B'' + (B'-4)(B'-3) + \frac{35}{9}\right)f_E^2\right], \qquad (4)$$

where $f_E = [(V_0/V)^{2/3}-1]/2$. Then, the heat capacity $C_{\rm v}$ can be obtained from

$$C_{\rm v} = 3nk\left[4D(\theta_{\rm D}/T) - \frac{3\theta_{\rm D}/T}{{\rm e}^{\theta_{\rm D}/T}-1}\right], \qquad (5)$$

$$\gamma = -\frac{{\rm d}\ln\theta_{\rm D}(V)}{{\rm d}\ln V}, \qquad (6)$$

where γ is the Grüneisen parameter, and $D(\theta_{\rm D}/T)$ represents the Debye integral, which can be described as

$$D(x) = \frac{3}{x^3}\int_0^x \frac{t^3}{{\rm e}^t - 1}{\rm d}t. \qquad (7)$$

A detailed description of this process can be found in Refs. [31], [33] and [34]. Using this method, we can successfully obtain the high-temperature and high-pressure properties of Mg_2Si.

3. Results and discussion

3.1. Benchmark calculation and elastic properties

To validate the performance of the PW-PP method, calculations on the lattice parameters and bulk modulus of anti-cotunnite and Ni_2In-type Mg_2Si are carried out at various pressures. The calculated results are listed in Table 1, together with the available experimental data.

Table 1. Calculated and experimental structural parameters for anti-cotunnite and Ni_2In-type Mg_2Si. (1 Å = 0.1 nm)

	Pnma				*P*6$_3$/*mmc*							
P/GPa	a/Å	b/Å	c/Å	B/GPa	P/GPa	a/Å	c/Å	a/Å	c/Å	P/GPa	*Pnma*	*P*6$_3$/*mmc*
7.5	6.695	3.925	7.771	82.6	21.9	4.339	5.495	4.308[a]	5.422[a]	0	B = 52.5 GPa[c]	B = 55.6 GPa[c]
10.4	6.535	3.929	7.688	91.9	24.1	4.319	5.459	4.280[a]	5.419[a]	0	B = 102.6 GPa[a]	B = 163.8 GPa[a]
14.5	6.364	3.906	7.596	106.9	27.6	4.287	5.410	4.278[a]	5.392[a]	0	56.6 GPa calc.	55.5 GPa calc
16.5	6.304	3.889	7.557	111.6	29.5	4.271	5.385	4.262[a]	5.388[a]			
20.2	6.197	3.865	7.483	120.5	34.6	4.231	5.322	4.231[a]	5.370[a]			
7.5	6.075[a]	4.646[a]	6.976[a]	84.1[b]	37.8	4.207	5.286	4.199[a]	5.304[a]			
10.4	6.051[a]	4.638[a]	6.892[a]	94.19[b]	40	4.192	5.263	4.166[a]	5.273[a]			
14.5	5.992[a]	4.624[a]	6.835[a]	108.2[b]								
16.5	5.973[a]	4.597[a]	6.790[a]	115.2[b]								
20.2	5.901[a]	4.583[a]	6.781[a]	127.5[b]								

[a] Ref. [19]; [b] Obtained by the vibrational Debye-like model; [c] Ref. [24];

As shown in Table 1, the calculated lattice constants and bulk moduli for anti-cotunnite Mg_2Si are in agreement with the experimental data. At 10.4 GPa, the average relative errors of the lattice constants a, b and c are 7.9%, –15.3% and 11.5%, respectively. In Ref. [24], the relative errors between the calculated lattice constants (at 10.4GPa) a, b, c and the experimental data are 8.9%, –13.8%, and 12.2%, respectively. More importantly, the relative errors between our calculated lattice constants (at 10.4 GPa) a, b, c and the values obtained by Yu *et al.*[24] are 0.9%, 1.6%, and 0.5%, respectively. In a pressure range of 7.5 GPa–20.2 GPa, our calculations overestimate the lattice constants a, c and underestimate b by 6.3%, 10.0% and –18.3%, respectively. This is in agreement with the results obtained by Yu *et al.*[24] (8.3%, 11.1% and –15.9%) . The agreement between our results and Yu's partially proves the validity of our calculation. For the Ni_2In-type Mg_2Si, the agreement between our calculated lattice constants and the values given in Ref. [19] is excellent in a pressure range of 21.9 GPa–40 GPa. At zero pressure and zero temperature, the calculated bulk moduli for anti-cotunnite and Ni_2In-type Mg_2Si are 56.6 GPa and 55.5 GPa, respectively. In Ref. [24], the calculated values are 52.5 GPa and 55.6 GPa. Hao *et al.*[19] have calculated the bulk modulus of Mg_2Si by Birch-Murnaghan EOS and the values for anti-cotunnite and Ni_2In-type Mg_2Si are 102.65 GPa and 163.83 GPa. There may be some errors in their calculations. The discrepancy between our calculated results and the experimental data originates mainly from the fact that (1) our calculated results are obtained at 0 K while the experimental data are measured at room temperature, and (2) the measurements of lattice constants are taken from polycrystalline samples with defects and porosity. However, in our calculation the Mg_2Si crystal is assumed to be defect-free under pressure.

Our results for the band structure of Mg_2Si are reported in Fig. 2 for some high-symmetry directions of the Brillouin zone. As shown in Fig. 2(a), the minimum of the conduction band is at the X point (0.229 eV) and the maximum of the valence band situated at the Γ point (0 eV). Therefore, the Mg_2Si crystal has a Γ_V–X_C indirect band gap (0.229 eV), which is in excellent agreement with the value 0.299 eV obtained by Chen *et al.*[35] We can also see from Fig. 1 that the valence bands can be divided into two parts. The valence bands below –5 eV are mainly composed of Si-s states. The second group of bands, which are located in an energy range of –5 eV–0 eV, is due mainly to Si-p states and Mg-p states. The conduction band

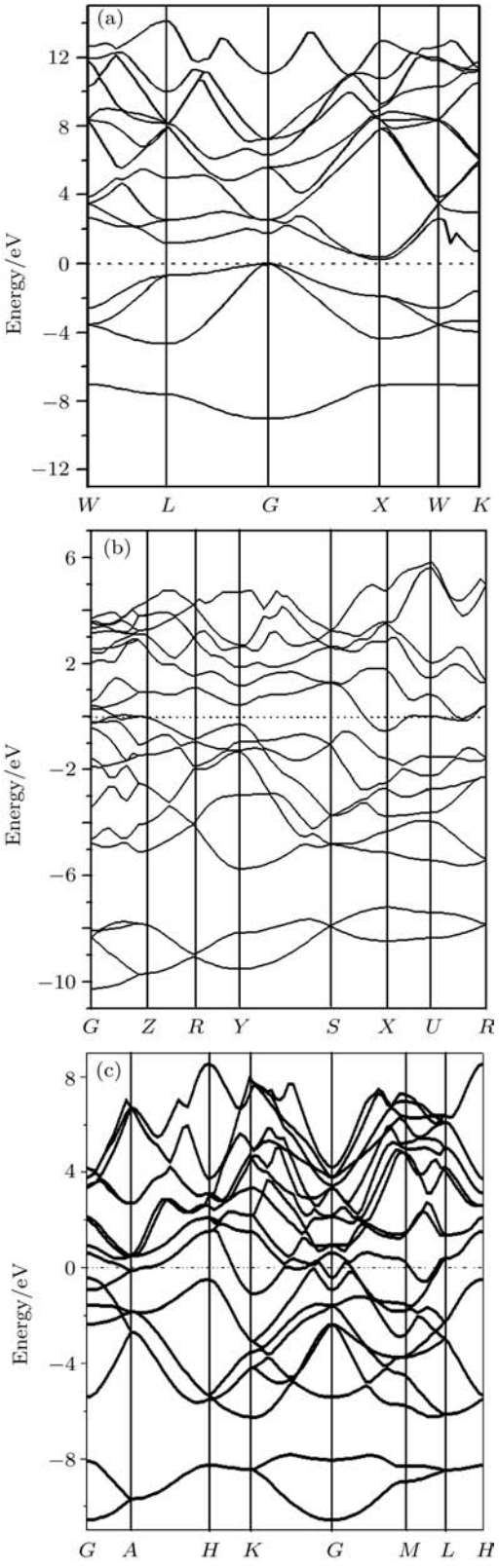


Fig. 2. Band structures of (a) anti-fluorite Mg_2Si , (b) anti-cotunnite Mg_2Si and (c) Ni_2In-type Mg_2Si, where G represents the Gamma point).

is a mixture of p and s states. The energy band gap between the valence and conduction bands at Γ point is 1.72 eV, which is smaller than the experimental value of 2.27 eV.[36] This underestimation is due mainly to the poor description of excited states in which the polarization effect is not accounted for by the exchange–correlation functional used in solving the Kohn–Sham equation.[37] Except for the value of the band gap, the overall features of our band structure topologically resemble the band structures reported in Refs. [4], [35] and [38], which means that they are in very good agreement with the experimental data.[39] Our result is consistent with the fact that anti-fluorite Mg_2Si is well known to be a small band gap semiconductor. As shown in Figs. 2(b) and 2(c), the band structures of the anti-cotunnite and Ni_2In-type Mg_2Si are more complicated and there is no clear band gap that can be seen. In Fig. 2(c), the valence band of the Ni_2In-type Mg_2Si is broadened to 10.5 eV. The valence band can also be divided into two parts (–10.5 eV to –7.5 eV and –7.5 eV to 0 eV), which are mainly contributed by Si-s, Si-p and Mg-p bands, respectively.

3.2. Phase transition

The phase transition characteristic of Mg_2Si is critical for checking the validity of the present calculations and to gain a deeper insight into the solid-state properties of this material. A theoretical estimate of the transition pressure from an anti-cotunnite to a Ni_2In-type structure can be obtained by the Gibbs free energy G ($\Delta G = G_{Pnma} - G_{P6_3/mmc}$) (Eq. (3)). The transition pressure can be determined via the corresponding ΔG–P curves calculated by the vibrational Debye-like model. The computed results are plotted in Fig. 3.

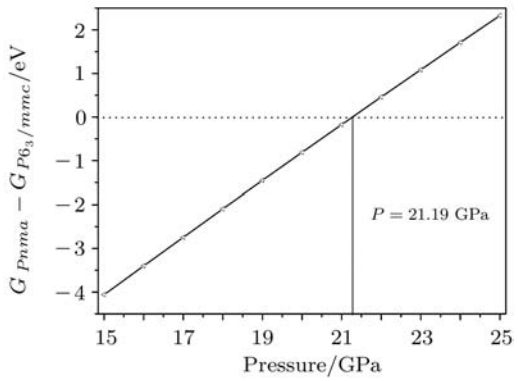


Fig. 3. Plots for Gibbs free energy difference versus pressure for anti-cotunnite and Ni_2In-type Mg_2Si at T = 300 K.

In Fig. 3, we illustrate the calculated curves of the Gibbs free energy difference as a function of the pressure P at which the temperature of these quantities are calculated. The pressure P at which the value of the Gibbs free energy difference is zero is the phase transition pressure. Accordingly, the two curves cross at 21.19 GPa, indicating a first-order phase transition. Beyond 21.19 GPa, the anti-cotunnite structure is more stable than the Ni_2In-type structure. In an earlier x-ray diffraction study,[19] the phase transition of Mg_2Si at room temperature was reported and the anti-cotunnite-to-Ni_2In-type phase transition was found to occur at 21.3 GPa. Using the CASTEP program, Yu *et al.*[24] have investigated the pressure-induced phase transition of Mg_2Si and calculated the transition pressure from anti-cotunnite structure to the Ni_2In-type structure to be 28.84 GPa ($T = 0$ K). Our calculated transition pressure is 24.12 GPa ($T = 0$ K), which is generally consistent with Yu *et al.*'s result. Therefore, our calculated transition pressure is in excellent agreement with the experimental value, and so our result is close to the experimental value compared with Yu's result.

Using the above-mentioned method, the phase boundary has been calculated and plotted in Fig. 4. The transition pressures from anti-cotunnite structure to Ni_2In-type structure are 24.12, 24.01, 23.93, 23.6, 23.02, 22.19, 21.19, 19.87, 18.46, 17.13, 15.56, 13.88 and 12.08 GPa, at temperatures of 0, 50, 100, 150, 200, 250, 300, 350, 400, 450, 500, 550, and 600 K, respectively. The transition pressure increases monotonically as the temperature rises. By fitting the P–T data points to a fourth order polynomial, the phase boundary can be described as

$$\begin{aligned} P = {} & 24.02994 + 3.93 \times 10^{-3}T - 4.66816 \times 10^{-5}T^2 \\ & - 2.2501 \times 10^{-9}T^3 + 2.33786 \times 10^{-11}T^4, \\ & T < 600K. \end{aligned} \tag{8}$$

Unfortunately, there are no theoretical results or experimental data available to check our calculated results. The calculated phase boundary should be testified by experimental and theoretical investigations in the near future.

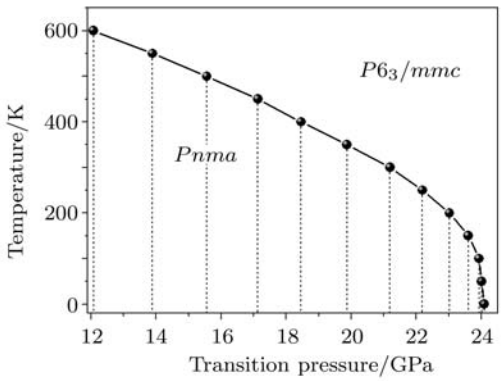


Fig. 4. Phase boundary between anti-cotunnite and Ni_2In-type Mg_2Si crystals.

3.3. High-pressure and high-temperature behaviours

Figure 5 shows the calculated values of thermal expansion α as functions of temperature and pressure applied separately to Ni_2In-type and anti-cotunnite Mg_2Si. Because the thermal expansion α has an anharmonic behaviour, one could not expect its linear variation with temperature. As can be seen in Fig. 5(a), below 200 K the thermal expansion rises sharply with temperature and increases slowly at high temperatures, as expected. We note that the temperature dependence of α for Ni_2In-type Mg_2Si is greater than for anti-cotunnite Mg_2Si, especially at high temperatures. At 300 K, the calculated thermal expansion coefficients are 3.23×10^{-6}/K and 1.31×10^{-6}/K for Ni_2In-type and anti-cotunnite Mg_2Si, respectively. For these two polymorphs, no experimental data or theoretical results are available to be compared with our results. As shown in Fig. 5(b), the phase transition involving a discontinuity in volume takes place at 21.19 GPa. At a given temperature, the thermal expansions of the two Mg_2Si polymorphs decrease strongly with pressure increasing, but the rates of slope differ from each other.

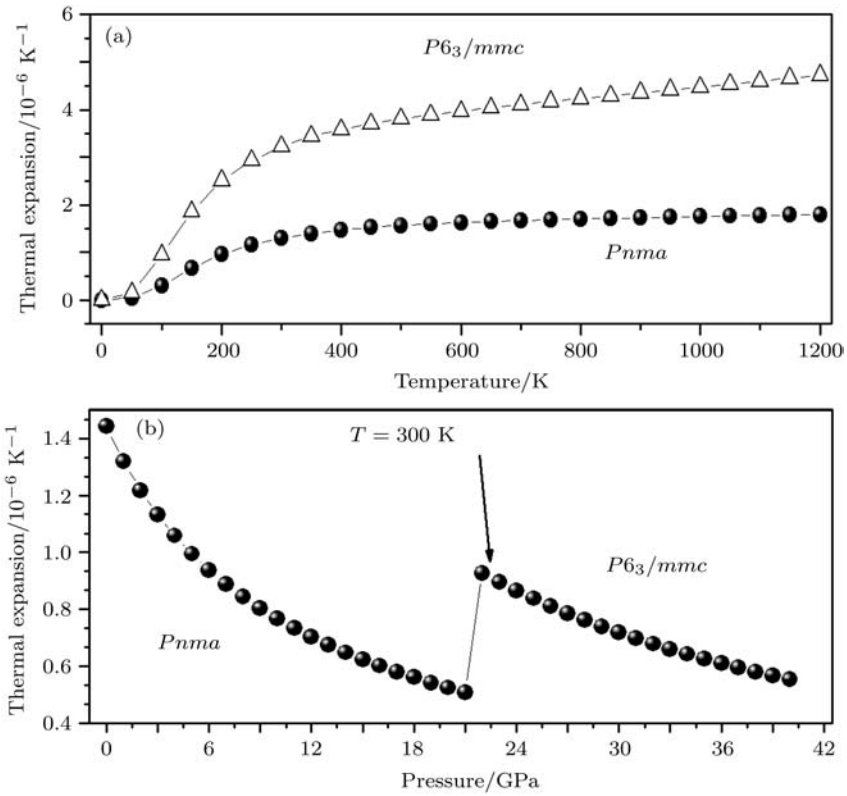


Fig. 5. Thermal expansions of Ni_2In-type and anti-cotunnite Mg_2Si each as a function of temperature at 0 GPa (a) and 300 K (b).

The temperature dependence of bulk modulus partially reflects the anharmonic interactions in solids because for a purely harmonic crystal the bulk modulus is independent of temperature. In order to acquire a good understanding of the effect of temperature and pressure on structural properties, we plot the variation of bulk modulus B with temperature in Fig. 6(a). It is clearly seen that as temperature T increases, the bulk modulus B decreases at 12 GPa, and the values of B at low temperatures are larger than at high temperatures for both Mg_2Si polymorphs. The variation in bulk modulus with temperature is small for anti-cotunnite Mg_2Si.

The temperature effect on Ni_2In-type Mg_2Si is greater than on anti-cotunnite Mg_2Si. At 12 GPa, a dramatic decrease can clearly be seen at approximately 600 K, indicating a phase transition occurring in the compound Mg_2Si. Figure 6(b) shows the computed bulk modulus variation versus pressure at 300 K. As expected, B increases monotonically with applied pressure. For both phases, the pressure effect on B is great. Our data also show a very small change in bulk modulus around 21.19 GPa, which is also believed to be due to a phase transition (see the inset). Applying the PW-PP method, the zero temperature bulk moduli for anti-cotunnite Mg_2Si are calculate to be 82.6, 91.9, 106.9, 111.6 and 120.5 GPa at pressures of 7.5, 10.4, 14.5, 16.5 and 20.2 GPa, respectively. The bulk moduli obtained by the vibrational Debye-like model are 83.1, 93.3, 108.2, 114.3 and 125.9 GPa respectively at those pressures. Using different methods, our calculated bulk moduli are in agreement with each other. To our knowledge, there is no research paper dealing with the bulk moduli of the Ni_2In-type and the anti-cotunnite Mg_2Si. So, so our computed results can make up for this lack of data.

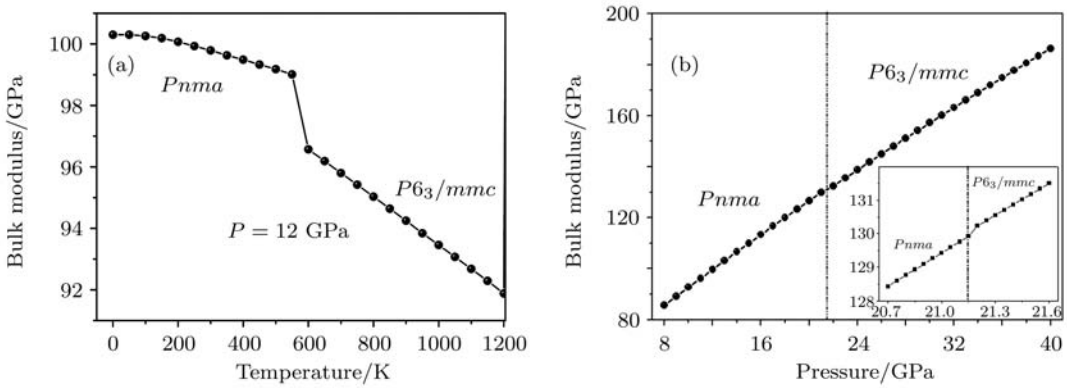


Fig. 6. Temperature dependences of bulk modulus B of Ni_2In-type and anti-cotunnite Mg_2Si at $P = 12$ GPa (a) and 300 K (b), where inset shows partial magnifications.

Knowledge of the heat capacity of materials not only provides a fundamental insight into their vibrational properties but is also mandatory for many applications. At intermediate temperatures, the temperature dependence of C_v is governed by the details of atom vibration and, for a long time, has only been able to be determined experimentally. In Fig. 7(a), we illustrate the temperature dependences of isochoric heat capacity C_v for anti-fluorite, anti-cotunnite and Ni_2In-type Mg_2Si at 0, 16 and 40 GPa, respectively. In order to testify the validity of the vibrational Debye-like model, we conduct another lattice dynamics calculation. The computed results are plotted in Fig. 7(b).

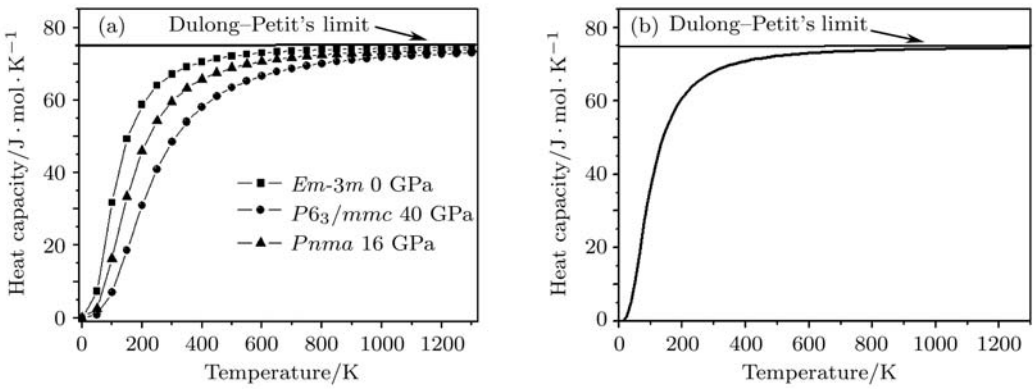


Fig. 7. Variations of heat capacity C_v for anti-fluorite, anti-cotunnite and Ni_2In-type Mg_2Si with temperature under three different pressures (a) and zero pressure (b).

As shown in Fig. 7(a), at low temperature C_v increases sharply with T and tends to zero when the temperature vanishes. This is due mainly to the anharmonic approximation of the Debye-like model used here. The temperature effect is much stronger than the pressure effect on C_v. At 0 GPa, the calculated heat capacities for anti-fluorite Mg_2Si at 50, 100, 150, 200, 250, 300, 400, 600, 800, 1000 and 1200 K are

7.32, 31.78, 49.78, 59.76, 64.73, 67.79, 70.49, 72.99, 73.84, 74.22 and 74.41 J·mol^{-1}·K^{-1}, respectively. Using the linear response method, the heat capacities for anti-fluorite Mg_2Si at those temperatures are calculated to be 11.51, 38.50, 53.01, 60.46, 65.25, 68.03, 70.94, 73.01, 73.77, 74.14 and 74.34 J·mol^{-1}·K^{-1}, respectively (see Fig. 7(b)). The heat capacities calculated by lattice dynamics and vibrational Debye-like model are in accordance with each other, which partially proves the validity of our vibrational Debye-like model. Our result accords well with the value obtained by Tani and Kido[22] (C_v = 67.9 J·mol^{-1}·K^{-1} at 300 K). The experimentally determined C_v at 50, 100, 200, and 300 K are 9.4, 33.8, 59.8, and 67.6 J·mol^{-1}·K^{-1}, respectively.[21] Our calculated results are also in excellent agreement with the above values. The heat capacity C_v of the anti-cotunnite Mg_2Si is greater than that of the Ni_2In-type Mg_2Si at the same temperature, but these two values are both smaller than the heat capacity of anti-fluorite Mg_2Si. At high pressures and temperatures, the anharmonic effects on C_v are suppressed. The temperature effect and the pressure effect on C_v are both small. The calculated heat capacities for three polymorphs are very close to Dulong–Petit's limit ($9Nk_B \approx 74.79$ J·mol^{-1}·K^{-1}), where N represents Avogadro's constant and k_B is the Boltzmann constant. Unfortunately, there are no experimental data or theoretical results available to be compared with our results.

4. Conclusions

We have performed first-principles calculations to investigate the structural, elastic and thermal properties of anti-cotunnite Mg_2Si and Ni_2In type Mg_2Si. The pressure dependences of the structural parameters and the bulk moduli have been systemically analysed. Then, the band structures of these polymorphs are calculated and analysed. Using the vibrational Debye-like model, the thermal expansions, the bulk moduli and the heat capacities of two Mg_2Si polymorphs are determined in a pressure range of 0–40 GPa and a temperature range of 0–1300 K. More importantly, our calculation method may be used to reproduce the phase transition characteristics from an anti-cotunnite structure to a Ni_2In-type structure. The phase boundary between these two phases is systemically investigated. To testify the validity of our calculation, we have calculated the heat capacity of anti-fluorite Mg_2Si by lattice dynamics. The C_v calculated by lattice dynamics is in agreement with the value obtained by vibrational Debye-like model. In this study a large amount of theoretical effort is made to explore the solid-state properties of Mg_2Si. The calculated results accord well with the experimental data and also the available theoretical results. Such consistence indicates that a vibrational Debye-like model combined with first-principles can accurately describe the high-temperature and the high-pressure behaviours of Mg_2Si.

Acknowledgements

The authors are grateful to Prof. M. A. Blanco and his coworkers for their GIBBS code, and also to Prof. P. Giannozzi and his colleagues for the QUANTUM ESPRESSO code.

References

[1] Okubo M, Ohishi T, Mishina A, Yanmauchi I, Udono H, Suemasu T, Matsuyama T and Tatsuoka H 2007 *Thin Solid Films* **515** 8268

[2] Saravanan R and Robert M C 2009 *J. Alloys Compd.* **479** 26

[3] Akasaka M, Lida T, Matsumoto A, Yamanaka K, Takanashi Y, Imai T and Hamada N 2008 *J. Appl. Phys.* **104** 013703

[4] Peng H, Wang C L, Li J C, Wang H C and Wang M X 2010 *Acta Phys. Sin.* **59** 4123 (in Chinese)

[5] Nolas G S, Wang D and Beekman M 2007 *Phys. Rev.* B **76** 235204

[6] Baleva M, Zlateva G, Atanassov A, Abrashev M and Goranova E 2005 *Phys. Rev.* B **72** 115330

[7] Tani J I and Kido H 2008 *Intermetallics* **16** 418

[8] Hachiya K, Goto T and Hagiwara R 2007 *Electrochim. Acta* **53** 46

[9] Chen Q, Xie Q, Yan W, Yang C and Zhao F 2008 *Sci. China* Ser. G **38** 825 (in Chinese)

[10] Yu Z, Xie Q, Xiao Q and Zhao K 2009 *Acta Phys. Sin.* **58** 6889 (in Chinese)

[11] Li C, Wu Y, Li H and Liu X 2009 *J. Alloys Compd.* **477** 212

[12] Zhao Y, Qin M J, Dou S X, Ionescu M and Munroe P 2006 *J. Appl. Phys.* **99** 08M503

[13] Wang X, Wang Y, Zou J, Zhang T, Mei Z, Guo Y, Xue Q, Du X, Zhang X, Han X and Zhang Z 2009 *Chin. Phys.* B **18** 3079

[14] Kunc K, Loa I and Syassen K 2008 *Phys. Rev.* B **77** 94110

[15] Duan Y H and Sorescu D C 2009 *Phys. Rev.* B **79** 014301

[16] Lazicki A, Yoo C S, Evans W J and Pickett W E 2006 *Phys. Rev.* B **73** 184120

[17] Kunc K, Loa I, Grzechnik A and Syassen K 2005 *Phys. Status Solidi* (b) **242** 1857

[18] Cannon P and Conlin E T 1964 *Science* **145** 487

[19] Hao J, Zou B, Zhu P, Cao C, Li Y, Liu D, Wang K, Lei W, Cui Q and Zou G 2009 *Solid State Commun.* **149** 689

[20] Liu N N, Song R B and Du D W 2009 *Chin. Phys.* B **18** 1979

[21] Gerstein B C, Jelinek F J, Habenschuss M, Schickell W D, Mullaly J R and Chung P L 1967 *J. Chem. Phys.* **47** 2109

[22] Tani J I and Kido H 2008 *Comput. Mater. Sci.* **42** 531

[23] Wang H, Jin H, Chu W and Guo Y 2010 *J. Alloys Compd.* **499** 68

[24] Yu F, Sun J X, Yang W, Tian R G and Ji G F 2010 *Solid State Commun.* **150** 620

[25] Yu B H, Chen D, Tang Q B, Wang C L and Shi D H 2010 *J. Phys. Chem. Solids* **71** 758

[26] Giannozzi P, Baroni S, Bonini N, et al. 2009 *J. Phys.*: *Condens. Matter* **21** 395502

[27] Vanderbilt D 1990 *Phys. Rev.* B **41** 7892

[28] Perdew J P, Burke K and Ernzerhof M 1996 *Phys. Rev. Lett.* **77** 3865

[29] Monkhorst H J and Pack J D 1976 *Phys. Rev.* B **13** 5188

[30] Baroni S, Gironcoli S De, Corso A D and Giannozzii P 2001 *Rev. Mod. Phys.* **73** 515

[31] Blanco M A, Francisco E and Luaña V 2004 *Comput. Phys. Commun.* **158** 57

[32] Murnaghan F D 1944 *Proc. Natl. Acad. Sci. U. S. A.* **30** 244

[33] Peng F, Liu Q, Fu H Z and Yang X D 2009 *Solid State Commun.* **149** 56

[34] Chen D, Chen J D, Zhao L H, Wang C L, Yu B H and Shi D H 2009 *Chin. Phys.* B **18** 738

[35] Chen Q, Xie Q, Yang C H and Zhao F J 2009 *Acta Opt. Sin.* **29** 229 (in Chinese)

[36] Baranek P, Schamps J and Noiret I 1997 *J. Phys. Chem.* B **101** 9147

[37] Baranek P and Schamps J 1999 *J. Phys. Chem.* B **103** 2601

[38] Kalarasse F and Bennecer B 2008 *J. Phys. Chem. Solids* **69** 1775

[39] Aymerich F and Mula G 1970 *Phys. Status Solidi* **42** 697